SIMPLIFIED DERIVATION OF ANGULAR ORDER AND DYNAMICS OF RODLIKE FLUOROPHORES IN MODELS AND MEMBRANES

Simultaneous Estimation of the Order and Fluidity Parameters for Diphenylhexatriene by Only Coupling Steady-State Illumination Polarization and Lifetime of Fluorescence

FRANÇOIS HARE
Centre de Recherche Paul Pascal, Domaine Universitaire, 33405 Talence Cedex, France

ABSTRACT We compare numerous values of average degrees of order, $\langle S \rangle$, and of average correlation times, $\langle \phi \rangle$, as given by many authors for 1-6-diphenyl-1-3-5-hexatriene (DPH) in membrane models. From these comparisons, a relationship arises between $\langle \phi \rangle$, $\langle S \rangle$, and the absolute temperature, T. This means that each of these three variables is a function of both the others: $\Omega [\langle \phi \rangle, \langle S \rangle, T] = 0$, and this function defines a surface in a three-dimensional space. Note that Ω seems identical for a large variety of sonicated lipid vesicles. This statement is a new formulation of the conclusions of Van Blitterswijk W. J., R. P. Van Hoeven, and B. W. Van Dermeer, 1981, *Biochim. Biophys. Acta,* 644:323–332, in the light of other recent studies (Kinosita K., Jr., R. Kataoka, Y. Kimura, O. Gotoh, and A. Ikegami, 1981, *Biochemistry,* 20:4270–4277). It seemed useful to seek an approximate analytical expression for the Ω function (supposed unique). Various arguments have led us to define the Ω function as the ratio of a diffusive (Arrhenius-type) numerator, $\nu_{(T)}$, divided by a temperature-independent denominator, $\sigma_{(\langle S \rangle)}$ (Kinosita, K., Jr., S. Kawato, and A. Ikegami, 1977, *Biophys. J.,* 20:289–305; Lipari, G., and A. Szabo, 1980, *Biophys. J.,* 30:489–506). However, one could not a priori discard a dependence of the activation energy of $\nu_{(T)}$ on both the temperature and/or on $\langle S \rangle$. The analytical form of the proposed approximate Ω function and the numerical values of the constants involved are checked for much of the data obtained from DPH/biomembranes systems described in the literature. As a consequence of this new relationship, a simplified procedure is proposed to obtain the order parameter, $\langle S \rangle$, in unknown systems. In this procedure the starting experimental quantities are only the steady-state fluorescence anisotropy, $\langle r \rangle$, the weighted average fluorescence lifetime, $\bar{\tau}$, and T. In turn, evaluation of a weighted average correlation time, $\langle \phi \rangle$, sometimes becomes simultaneously possible, at least for membranes in their liquid-crystal phase, but with less accuracy than for the determination of $\langle S \rangle$. Because the method is founded on results arising from transient experiments, it seems difficult to conceive that it could replace these techniques in a generalized manner. However, because fast tests are frequently required in routine studies on biomembranes, the method could still have a broad application provided that some transient-control measurements are performed at the limits of the experimental range studied.

INTRODUCTION

General Expressions for Transient Intensity and Anisotropy of Fluorescence

In experiments where a rod-shaped dye lies in an uniaxial environment, the most often performed transient measurements are the responses of both the trace, $\mathcal{F}(t)$, and the anisotropy, $r(t)$, of the emission tensor to a δ-shaped excitation. They allow us to obtain a representation of the equilibrium distribution and of the dye dynamical behavior of the dye-medium interactions, respectively, by the order parameter $\langle s \rangle$ and by the average reorientational time $\langle \phi \rangle$ of the probe. In recent works (1, 2) experimental interdependence of $\langle s \rangle$ and $\langle \phi \rangle$ is underlined and such a correlation is developed here.

The quantities $r(t)$ and $\mathcal{F}(t)$ are obatined by a variety of means, including deconvolution computation procedures. Multiexponential decays are frequently observed for $\mathcal{F}(t)$, while $r(t)$ exhibits a similar decay form with, however, an added constant (3, 4, 5, 6) r_∞ that is zero only when the

A preliminary account of this work was presented at the International Workshop on Fluorescence and Membrane Markers in Immunology and Cancerology in Montpellier, France, on December 14 and 15, 1981 (see reference 38).

medium is isotropic

$$\mathcal{F}(t) = \Sigma_j \alpha_j \cdot \exp(-t/\tau_j) \quad (1)$$

$$r(t) = r_\infty + \Sigma_i \beta_i \cdot \exp(-t/\phi_i). \quad (2)$$

Four classes of parameters are consequently known at this stage, the sets of the α_j, τ_j, β_i (with r_∞), and ϕ_i (5–8). The following causes may reduce the number of parameters. First, from an experimental point of view, it is difficult to resolve $\mathcal{F}(t)$ and $[r(t) - r_\infty]$ when they contain two or three exponentials. This is not easy in time-resolved polarized fluorescence experiments with pulse excitation (TRPF), and becomes a very hard task, particularly for $[r(t) - r_\infty]$, with the phase and demodulation technique. Second, only the parameters describing $r(t)$ are significant for structural studies (order and dynamics); those that govern the decay of $\mathcal{F}(t)$ are concerned with the photophysical properties of the dye itself (energies of fundamental and excited conformational states). Third, some consideration of the symmetry of the dye molecule and of the surrounding medium allows us to reduce the predicted number of exponential functions, which describe the decrease of $r(t)$ for anisotropic (7, 9–11) and isotropic (12) probe environments.

Simplified Formalism

On these grounds (in the case of a rod-shaped dye lying in an uniaxial environment and provided that the additional conditions discussed below are fulfilled), many authors retain a simplified phenomenological formalism for $r(t)$ (2, 3, 13–15) that is macroscopically exact only in particular situations

$$r(t) = r_\infty + (r_0 - r_\infty) \exp(-t/\phi). \quad (3)$$

This simple relation does not hold true in every case. For instance, Szabo (9) as well as Zannoni (10) point out that at an experimental level, two apparent relaxation times may be extracted from $r(t)$; the first one ($t \to 0$) contains dynamical contributions only, the second one $\int_0^\infty r(t)$ ($[\int_0^\infty r(t)\,dt - r_\infty]$ is exact) dt further contains the order (equilibrium for t_∞). Moreover, at the theoretical level and within a truly uniaxial medium, the relation (Eq. 3) can be rigorously demonstrated in the frame of a large jump collision model for the microscopic diffusion (strong diffusion model). On the contrary, in the frame of a very small-jump collision model (Brownian diffusion), decays containing several exponentials are predicted for any shape of hindering orientational potential. For instance, the number of exponentials is three in the case of a rod-shaped dye surrounded by an uniaxial medium, provided that its absorption and emission moments lie along its principal molecular axis (7, 10).

In conclusion, to prove the validity of the relation (Eq. 3), we emphasize that Eq. 3 can be taken as an approximation of the relation in Eq. 2 (general solution for the Brownian diffusion) in at least three cases: (*a*) a Maier Saupe hindering potential under the condition $0.3 \leq S \leq 0.7$ (11), (*b*) a rectangular hindering potential that leads to the solution of the diffusion equation that enables the replacement of ϕ by an average, correctly chosen, $\langle\phi\rangle$. When this replacement is performed in Eq. 3, the exact approach of Eq. 2 is obtained in three limiting situations (4), $t = 0$, $t \to \infty$, and $\int_0^\infty r(t)\,dt$ having the exact value. (*c*) The third condition is arbitrary (other choices are possible) (4), but it is advantageous because it leads (3, 4) to a very simple expression for $\langle\phi\rangle$

$$\langle\phi\rangle = \Sigma_i \frac{\beta_i \phi_i}{1 - r_\infty}. \quad (4)$$

Lack of Complete Identity Between a Membrane and a Uniaxial Medium

Now, one must examine the consequences of the relations (Eqs. 2–4) on the expression of the steady-state anisotropy $\langle r\rangle$. Before looking into this point, it must be remarked that the above models of diffusion were built depicting a true uniaxial environment for the probes. Some restrictions remain that lead us to believe that this whole treatment can only be a rough description of phospholipid vesicles or membranes for at least three reasons. (*a*) There is a gradient of order along the local normal to the bilayer (16–20) (z-axis of the director [9, 11]). (*b*) The radius of curvature of the bilayer has a finite value and this medium is consequently at least biaxial. This corresponds to the splay distortion in a nematic liquid crystal (21). (*c*) To a lesser degree, the extension of the medium along the z-axis of the director is finite, in contrast with that of a liquid crystal. These three limitations may explain that theoretical predictions, which hold true for multiple-domain liquid crystals (particularly σ functions as defined below), are only approximated for experiments with lipid vesicles.

Emission Anisotropy Under Steady-State Illumination

Now, to deduce $\langle r\rangle$ from the relations in Eqs. 2 and 3, a series of Carson-Laplace transforms must be performed as follows

$$\langle r\rangle = \frac{\int_0^\infty \mathcal{F}(t) \cdot r(t) \cdot dt}{\int_0^\infty \mathcal{F}(t) \cdot dt} \quad (5)$$

(5, 10), which gives

$$\langle r\rangle = \frac{1}{\Sigma_j \alpha_j \tau_j} \int_0^\infty \sum_{ij} \cdot [r_\infty + \beta_i \exp(-t/\phi_i)] \times [\alpha_j \exp(-t/\tau_j)]\,dt \quad (6)$$

$$\langle r \rangle = r_\infty + \frac{1}{\Sigma_j \alpha_j \tau_j} \sum_{ij} \frac{\alpha_j \beta_i}{\frac{1}{\tau_j} + \frac{1}{\phi_i}} \tag{7}$$

(see reference 22).

Provided that either (*a*) $[r(t) - r_\infty]$ or (*b*) $\mathcal{I}(t)$ can be described by a single exponential function, Eq. 7 can be reduced. Case *a* proves that Eq. 3 is valid; and if we only consider $j = 1,2$ (see, i.e., reference 22), and define

$$\bar{\tau} = \Sigma_j \alpha_j \tau_j = \alpha_1 \tau_1 + \alpha_2 \tau_2, \tag{8}$$

then

$$\langle r \rangle = r_\infty + \left(\frac{r_0 - r_\infty}{\bar{\tau}} \right) \left(\frac{\alpha_1}{\frac{1}{\tau_1} + \frac{1}{\phi}} + \frac{\alpha_2}{\frac{1}{\tau_2} + \frac{1}{\phi}} \right). \tag{9}$$

In case *b*, if we only consider $i = 1, 2$

$$\langle r \rangle = r_\infty + \frac{\beta_1}{1 + \frac{\tau}{\phi_1}} + \frac{\beta_2}{1 + \frac{\tau}{\phi_2}}. \tag{10}$$

The very simplified relation

$$\langle r \rangle = r_\infty + \frac{r_0 - r_\infty}{1 + \frac{\tau}{\phi}} \tag{11}$$

strictly holds true only when $\mathcal{I}(t)$ is a monoexponential and $[r(t) - r_\infty]$ is also a monoexponential, i.e., $\tau_{1,2} \equiv \tau$, and $\phi_{1,2} \equiv \phi$, simultaneously.

Distinct Values of ϕ, $\langle \phi \rangle$, and of the Various $\bar{\phi}_{app}$[1]

Various approximate values, $\bar{\phi}_{app}$, are often introduced (Eq. 11) keeping this very simple form in situations in which Eq. 3 does not strictly hold. Even with a single τ, replacement of ϕ in Eq. 11 by expressions such as those found in the literature (3, 4, 8, 22) is not rigorous. Neither

$$\bar{\phi}_{harm} = \Sigma_i \beta_i \cdot \left(\sum_i \frac{\beta_i}{\phi_i} \right)^{-1} \tag{12}$$

(4) nor

$$\bar{\phi} = \frac{\Sigma_i \beta_i \phi_i}{\Sigma_i \beta_i} \tag{13}$$

are equivalent to the use of Eq. 10.

Similarly, even in the case of a single ϕ (condition of validity of Eq. 3), replacement of τ in Eq. 11 by some approximate expression such as either Eq. 8 (22) or

$$\langle \tau_{moments} \rangle = \bar{\tau}^{-1} \times \int_0^\infty t \cdot \mathcal{I}(t) \cdot dt = \frac{\alpha_1 \tau_1^2 + \alpha_2 \tau_2^2}{\alpha_1 \tau_1 + \alpha_2 \tau_2} \tag{14}$$

(8) is not equivalent to the use of Eq. 10. In fact, because the proposition "$\int_0^\infty r(t)\, dt$ is exact" was used above to define $\langle \phi \rangle$ in the case of a modelized rectangular potential, in a similar manner the proposition $\langle r \rangle$ is exact in Eqs. 5 and 7 defines another kind of average, $\bar{\phi}$, which could hold in Eq. 3. However this last average is no longer appropriate for expressing ϕ in Eq. 11.

In the following, we shall interpret the experiments described in the literature only in terms of Eqs. 3 and 11. We choose to take a rough approach to the systems discussed in this paper and to look for correlations between dynamics and order. Concerning the use of Eq. 3, let us recall that in reference 4, for instance, the authors emphasize that any distinction between Eqs. 2 and 3 becomes virtually impossible for $\langle \phi \rangle = (\Sigma_i \beta_i \phi_i)/(1 - r_\infty)$ as soon as $r_\infty > 0.083$. We shall call the supposedly unique experimental correlation time, $\langle \phi \rangle$. Because of the numerous accumulated approximations (particularly since the order gradient and the vesicle curvature were neglected), this single $\langle \phi \rangle$ (which is obtained by experiment) cannot exactly satisfy the conditions for the uniaxial model. With regard to Eq. 11 we emphasize that this relation becomes phenomenologically invalid whenever $\mathcal{I}(t)$ is no longer a monoexponential. Clearly it becomes impossible to find a value of $\langle \tau \rangle$, which contains only $\alpha_1, \alpha_2, \tau_1, \tau_2$, that can replace τ in Eq. 11 and still allow τ to retain the exact character as in Eq. 10 (such a $\langle \tau \rangle$ necessarily mixes α_j, τ_j, and $\langle \phi \rangle$). In spite of this, and to make it simpler, we will use Eq. 11 in an approximate manner, keeping the definition of Eq. 8 rather than that of Eq. 14 for $\langle \tau \rangle$.

Comparison with Other Methods

Various alternative methods have been proposed for extraction of the microscopic parameters $\langle S \rangle$ and $\langle \phi \rangle$, from the observable quantity, $\langle r \rangle$. One of them allows us to measure r_∞ starting from lifetime measurements, and $\langle r \rangle$ only; it is the so-called lifetime-resolved methodology (Lakowicz and co-workers [23–26]). Complete transient study of $r(t)$ is avoided, as it is here. It is replaced by the study of the influence of an additional species (the quencher), introduced in the medium at various concentrations. This induces changes of $\langle r \rangle$ that are coupled with decreases of the lifetime values (or, in some simple appropriate cases, with decreases of the steady-state intensity $\langle \mathcal{I} \rangle$). So, plots of $([r_0 - \langle r \rangle]/\tau)$ vs. the quencher concentration yield r_∞, and then ϕ. This procedure reduces the need for time-resolved measurements and therefore allows a gain in experimental time, although a rather large number of measurements are necessary for extrapolation. However, the presence of the quencher may introduce some additional perturbations in the system.

[1]This discussion was added to satisfy the reviewers' requirements. I wish to thank them for encouraging me to clarify these points and for directing me to a more complete bibliography.

Relative Importance of Dynamics and Order as Compared During the Last Decade

Several recent works (3, 4, 7, 27) emphasize that the different orientational correlation times, ϕ_i, and in turn $\langle\phi\rangle$, contain a strong contribution of the equilibrium (infinite time) angular distribution of the rod molecules; the dynamics of the population depends on r_∞, which can be related to the limit angle that this population will reach at infinite time. We note that during the last few years, the diffusive part of the ϕ_i's (their true dynamical part), relative to a uniaxial environment, has been playing a less and less important role in the interpretation of these data while, at the same time, the order parameter $\langle S\rangle$ (describing an equilibrium state) has become more prevalent; i.e., the original concept of microviscosity corresponding to the use of Eq. 11 with $r_\infty = 0$ (28–31) has been modified. By analogy, similar conclusions have been drawn about the comparative effects of the intrinsic parameters of the lipid chains (respectively, the order parameter, $\langle S^{CH_2-CH_2}\rangle$, and the viscosity, $\langle\eta^{CH_2-CH_2}\rangle$) on the orientation, and on the motion of the nonlipid intrinsic components of the membranes, the proteins, for example.

This last conclusion cannot be definitive; even if the limiting angular distribution governs the rotational relaxation, in the case of probes containing ~14–20 carbon atoms, it is not established that this will hold true for much larger species such as proteins moving in the membranes. For instance, although depolarized fluorescence experiments performed with rod-shaped dyes often show that $\langle S^{probe}\rangle$ is the prevalent factor in $\langle r\rangle$ (often much more important than the diffusion), the relative weights of each of these causes might be reversed in interpretation of the motion of more or less immersed proteins. If such a hypothesis were correct, one could understand why the equilibrium angular distribution of the

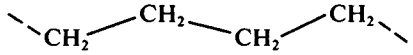

chains (approximated by $\langle S^{probe}\rangle$) might predict, although indirectly, the mobility of proteins, as was the case in Shinitzky's methodology, although this last author implicitly assumed that $r_\infty = 0$. However, one must emphasize that the ϕ_i's, and in turn $\langle\phi\rangle$, also contain a diffusive component (2, 3, 4). This can be expressed by using an Arrhenius function, which determines the main response of $\langle\phi\rangle$ to variations of temperature in thermal ranges in which S varies slowly (i.e., far from any thermal-phase transition). In isotropic liquids, the Arrhenius term surely reflects the fluid behavior. However, it is more difficult to interpret in uniaxial media.

In what follows, we first discuss the problems of the form and the dependence of the ϕ_i's (and, in turn, of $\langle\phi\rangle$) on $\langle S\rangle$ and on the temperature. A considerable experimental simplification would be obtained if the relation, $\Omega(\langle\phi\rangle, \langle S\rangle, T) = 0$, could be the same for any membrane systems. Second, we discuss whether or not the Arrhenius term in $\langle\phi\rangle$ is dependent on the order. This particular point questions the true dynamical nature of the diffusion coefficient obtained in an uniaxial medium, as well as the hydrodynamical interpretation, i.e., the so-called fluidity and microviscosity, even taken in the cone.

BASIC RELATIONSHIPS BETWEEN $\langle\phi\rangle$, $\langle S\rangle$, T

(*a*) Defining θ_{lim} as the angle between the z-axis of the uniaxial membrane director and the z_{Mol}-axis of an arbitrarily oriented rod molecule in the equilibrium distribution $f(\theta_{lim})$, the degree of order $\langle S\rangle$ is the second moment of this distribution and takes the form: $\langle \mathcal{D}^{(2)}_{00}(\cos\theta_{lim})\rangle$, the central element of the second-rank Wigner matrix, which is also equivalent to the second-order Legendre polynomial, $\langle P_2(\cos\theta_{lim})\rangle$ (9–11, 27, 32, 33–36).

It can be demonstrated (10, 27) that, under the conditions of macroscopic isotropy, the fundamental and limiting fluorescence anisotropies, r_0 and r_∞, are related to $\langle S\rangle$ by

$$\frac{r_\infty}{r_0} = \langle S\rangle^2 \times \left[\frac{P_2(\cos\beta_a)\cdot P_2(\cos\beta_e)}{P_2(\cos\beta_{ae})}\right] \qquad (15)$$

in which the angles are defined by the absorption and emission moments μ_a and μ_e, respectively, as

$$\cos\beta_a = (z_{Mol}\cdot\mu_a),\ \cos\beta_e = (z_{Mol}\cdot\mu_e),\ \text{and}\ \cos\beta_{ae} = (\mu_a\cdot\mu_e).$$

Under the additional condition that either μ_a or μ_e lies along z_{Mol}, Eq. 15 gives

$$\langle S\rangle = \left(\frac{r_\infty}{r_0}\right)^{1/2} = \frac{3\langle\cos^2\theta_{lim}\rangle - 1}{2}. \qquad (16)$$

In that case, both moments do not have to be aligned (10).

Eq. 16 holds true for macroscopically isotropic systems such as multiple domain liquid crystals and vesicle suspensions. Inaccuracies in the determination of $\langle S\rangle$ arise from errors in both r_0 and r_∞. The first of these quantities is determined either by steady-state depolarization in glassy solvents or by checking r_0 in a time-resolved experiment. In the last case, two procedures are commonly used, (*i*) fixing r_0 at the value determined in glassy solvents, and (*ii*) letting it run as a free parameter. In case *ii*, one frequently obtains values that are lower than those determined in glasses (15, 28). Some residual scattering of the exciting beam (37) must always be suspected in experiments on vesicle suspensions and could provide a possible explanation. A high degree of indeterminacy obtains at this stage. The measure of r_∞ also causes some inaccuracy in $\langle S\rangle$, as in the following examples. First, in TRPF, the noise at long times associated with the observed intensities $\mathcal{I}^{\parallel}$ and $\mathcal{I}^{\perp}$ (respectively parallel and perpendicular to the exciting electric field) increases the relative error in r_∞. For the case in which Eq. 11 is valid and in an ideal experiment where

the exciting flash exhibits no tail, deconvolution is not necessary to derive r_∞. In practice, however, this tail cannot be avoided in at least the majority of current-flash fluorometers, and the undeconvoluted ratio, $(\mathcal{I}^{\parallel} - \mathcal{I}^{\perp})/(\mathcal{I}^{\parallel} + 2\mathcal{I}^{\perp})$, tends towards $\langle r \rangle$ at long times, so that deconvolution is always necessary. Consequently, small values of $\langle S \rangle$ are difficult to evaluate. Second, in phase and modulation measurements, many experimental difficulties arise when the rotation is very slow. A good example is the situation in which the hindering torque of the solvent relaxes very slowly as compared with the initial local relaxation rate, $1/\langle \phi_0 \rangle$. Despite the fact that this case is testable in principle by measurements at several frequencies, one encounters very great difficulties in distinguishing between equilibrium anisotropy (order) and two-step relaxation, when one of these steps is very slow (F. Hare and J. F. Faucon, unpublished results).

(*b*) Derivation of the reorientational diffusion coefficient, $D_\perp$, from the above described quantities ($\langle \phi \rangle$ and $\langle S \rangle$) requires in addition the knowledge of the function, $\sigma_{(\langle S \rangle)}$, defined as the ratio $(D_\perp/6R_\perp)$, where $6R_\perp = \phi^{-1}$ in which ϕ is obtained by an analysis of TRPF data using Eq. 3 (3). In fact, $\sigma_{(\langle S \rangle)}$ cannot be obtained without the help of a model of collisions (3, 4) and is obviously model dependent. In cases in which Eq. 3 can be taken as a satisfactory approximation, this function, σ, has been calculated for different symmetries of probes and different forms of hindering potentials (3, 4, 7). Its use in Eq. 11 must be considered with all the restrictions we have underlined in the Introduction, because σ has been defined for $\langle \phi \rangle$, not for $\bar{\phi}$. Various approximate analytical forms have been used for σ (2–4, 7). In all the models analyzed in the literature, the functions $\sigma(\langle S \rangle)$ obtained pass through the value zero for $\langle S \rangle = 1$. This seems to imply that $\langle \phi \rangle \to \infty$ when $\langle S \rangle \to 1$, except in the case when $D_\perp \to 0$. When temperature is the cause of the variations of $\langle S \rangle$ (Figs. 1–3), one observes the opposite of this prediction. If other causes alone are implied (e.g., cholesterol content), the conclusion of the models may still hold true.

FURTHER RELATIONSHIPS BETWEEN THESE QUANTITIES

From thermodynamical and kinetic considerations, Shinitzky predicted another kind of relationship between mobility and order (28, 30, 31). This author and his co-workers assumed that the activation energy of $6R_\perp$ was an appropriate function of $\langle S \rangle$ (30, 31). Recently, attempts have been made in three important works to determine such relationships. Kinosita et al. (2) and Stubbs et al. (22) tried to eliminate temperature by combining separated thermal variations of $D_\perp$ and of $\langle S \rangle$, which they obtained in various model and real membranes (Fig. 3 in reference 2). Although the authors do not stress it, the graph presented $\{\langle S \rangle, D_\perp\}$ is not a curve, but a surface; T still remains a variable of the system, as will be shown below. However, the authors clearly show that $D_\perp$ is a function of $\langle S \rangle$ (Fig. 3 in reference 22). Further, Van Blitterswijk et al. (1) try to minimize the influence of the fluorescence lifetime, $\bar{\tau}$, and to eliminate simultaneously the temperature between thermal variations of the following parameters: r_∞ (related to $\langle S \rangle$) and the fluorescence anisotropy under steady-state illumination, $\langle r \rangle$, which are related by

$$\frac{\langle r \rangle}{r_0} - \frac{r_\infty}{r_0} = \frac{1 - \langle S \rangle^2}{1 + \dfrac{\bar{\tau}}{\langle \phi \rangle}} \leftrightarrow \frac{\langle r \rangle}{r_0} = \langle S \rangle^2 + \frac{1 - \langle S \rangle^2}{1 + \dfrac{\bar{\tau}}{\langle \phi \rangle}}. \quad (17)$$

In this last work too, it is easy to show (see below) that the relation they have found will change with change in temperature. In fact, the problem is strictly the same in these three papers. We have proposed a new approach to this question (38) and have shown that it leads to an experimental simplification in determining the bilayer parameters. We shall discuss our method with the help of experimental results on model membranes extracted from the literature. Then, we shall give the first results obtained with data from membrane systems currently at hand. All following values of $\langle S^{\text{probe}} \rangle$ and of $\langle \phi^{\text{probe}} \rangle$ henceforth designated by S and $\langle \phi \rangle$, respectively, are relative to diphenylhexatriene, DPH.

GRAPH OF $1/\langle \phi \rangle$ VS. S

Van Blitterswijk et al. (1) plotted

$$\left.\begin{aligned} &\text{either } \frac{r_\infty}{r_0} \text{ vs. } \frac{\langle r \rangle}{r_0}, \text{ i.e., } S^2 \text{vs.} \left[S^2 + \frac{(1 - S^2)}{\left(1 - \dfrac{\bar{\tau}}{\langle \phi \rangle}\right)} \right] \\ &\text{or } \frac{\langle r \rangle - r_\infty}{r_0} \text{ vs. } \frac{\langle r \rangle}{r_0}, \text{ i.e., } \frac{1 - S^2}{\left(1 - \dfrac{\bar{\tau}}{\langle \phi \rangle}\right)} \text{vs.} \left[S^2 + \frac{(1 - S^2)}{\left(1 - \dfrac{\bar{\tau}}{\langle \phi \rangle}\right)} \right] \end{aligned}\right\}$$

At first, instead of these coordinates, we choose a more eloquent and more accurate representation, the plot of $1/\langle \phi \rangle$ vs. S (we compared this with the Kinosita et al. coordinate system $[\theta_c, D_\perp]$). The points that were compacted in the $(r_\infty/r_0; \langle r \rangle/r_0)$ plots now define three successive sheets relative to dipalmitoyl, dimyristoyl, and dioleyl plus natural egg phosphatidylcholines in the same sheet (DPPC, DMPC, DOPC, EPC, respectively) as visualized in Fig. 1.

Taking into account the corresponding values of $\bar{\tau}$ (Fig. 2), one observes that these three principal sheets remain discriminated, while neither the theoretical nor the experimental comprehensive fit of Van Blitterswijk et al. can describe all cases studied. In some particular systems, e.g., 3:1 DMPC/cholesterol, a system interpreted from Lakowicz et al. (15), very serious discrepancies appear (Fig. 3). This system exhibits another kind of relationship between S and $D_\perp$. This leads us to think the fits of previous authors (1, 33) are only a first approximation (Fig. 3 *b*).

Now, we shall discuss the consequences of the discrepan-

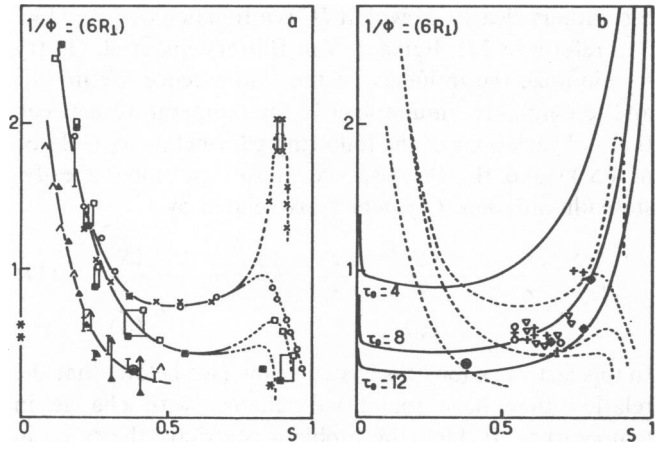

FIGURE 1 (*a*) Effective scattering of the results compacted in reference 1. Although the authors of reference 1 have collected data from a great number of works, the points corresponding to the phospholipids lie along three main sheets. This fact was not evident with the authors' type of representation. (*b*) Comparison between the experimental results (Fig. 1 *a*) and the theoretical fit proposed in reference 1. (See --- in Fig. 1 *a*, for comparison.) The authors have proposed $\tau/\phi = \gamma_0^{-1} \cdot (1 + S)/[(1 - S) \cdot (1 + 2S)]$ with $\gamma_0^{-1} \geq 4$; this amounts to taking $\tau/\phi = [(D_0\tau_0)/(6)] (1 + S)/[\frac{1}{8} (1 - S) \cdot (1 + 2S)]$, with $(D_0\tau_0)/(6) = \gamma_0^{-1}$. A single adjustable parameter, τ_0, remains.

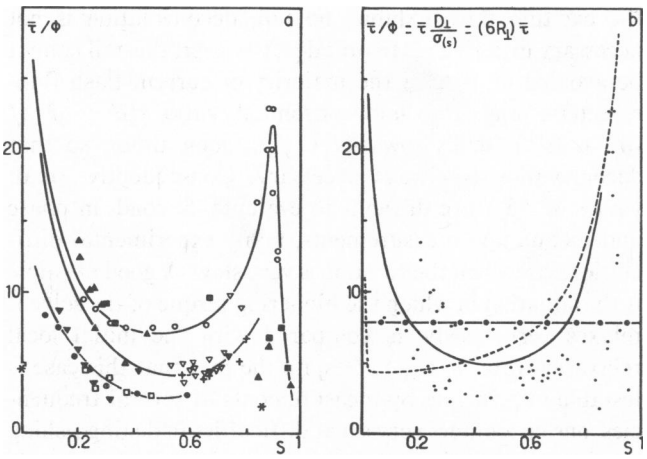

FIGURE 2 (*a*) Conversion of the three sheets of Fig. 1, taking into account the experimental values of $\bar{\tau}$; the three main curves remain distinct. □, EPC (from reference 8); *, DMPC (from reference 5); ▲, DMPC (from reference 15); ▼ and ●, DOPC (from reference 15); ○, DPPC (from reference 6); ■, DPPC (from reference 15); +, membranes and ▽, models from reference 39. (*b*) Comparison between the experimental results in Fig. 2 *a* and various fits, Van Blitterswijk's fit and Jähnig's fit. For Van Blitterswijk, the experimental fit, ——, in reference 1 corresponds to the average curve drawn across the data reviewed in Fig. 1 *a*, as indicated by · · · . The theoretical fit, ---, corresponds to that of Fig. 1 *b* above. — · —, Jähnig's fit ($\bar{\tau}/\phi = 8$).

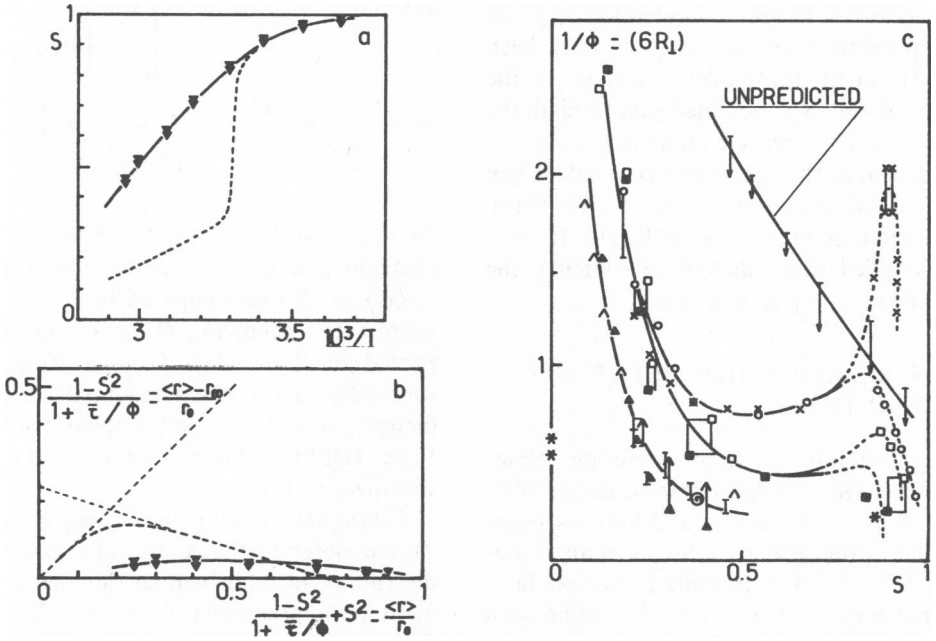

FIGURE 3 A typical example of systems for which the previously proposed fits are irrelevant (nonconforming system). A 3:1 DMPC/cholesterol system interpreted from Lakowicz et al. (reference 15) is illustrated. (*a*) Data points indicate thermal variation of the degree of order. ---, indicates thermal variation of the degree of order for pure DMPC. (*b*) The same system in Van Blitterswijk et al. coordinates system. ---, the average experimental fit of these authors; the lack of compliance with their unique curve is observable. (*c*) Unpredicted, the same system as in Fig. 3 *b* plotted in the coordinates system proposed in the present report. The observed variation of $\langle\phi\rangle^{-1}$ is the opposite of that predicted by models when one uses a σ function that passes through zero when $S = 1$. Other curves are those of Fig. 1 *a* and are drawn for comparison.

cies in $1/\langle\phi\rangle$ and in $\bar{\tau}/\langle\phi\rangle$, and how $\langle r\rangle$ (and the estimation of r_∞ starting from $\langle r\rangle$) will be affected. If both the parts of $\langle r\rangle$ are considered (Eq. 11), it appears that they can be redistributed in various manners, e.g.,

$$\langle r\rangle = \frac{r_0}{1+\bar{\tau}/\langle\phi\rangle} + \frac{r_\infty}{1+\langle\phi\rangle/\bar{\tau}},$$

$$r_\infty = \langle r\rangle - \frac{\langle\phi\rangle}{\bar{\tau}}\cdot(r_0 - \langle r\rangle), \tag{18}$$

which immediately gives

$$S = \left[\frac{\langle r\rangle}{r_0} - \frac{\langle\phi\rangle}{\bar{\tau}}\cdot\left(1 - \frac{\langle r\rangle}{r_0}\right)\right]^{1/2}. \tag{19}$$

Eq. 19 can replace Eq. 16 when one wants to use $\langle r\rangle/r_0$ instead of r_∞/r_0.

At one of the two limits of the range of variation of $\langle r\rangle$, an approximate form of Eq. 19 can be very useful when $\langle r\rangle \to 0$,

$$S \simeq \left[\frac{\langle r\rangle}{r_0} - \frac{\langle\phi\rangle}{\bar{\tau}}\right]^{1/2}. \tag{20}$$

On the other hand, at the other limit, the situation remains ambiguous when $\langle r\rangle \to r_0$, either $\langle\phi\rangle$ does not increase very much ($\bar{\tau}/\langle\phi\rangle$ increases, remains constant, or decreases slowly) so that $S \to (\langle r\rangle/r_0)^{1/2}$, or $\langle\phi\rangle$ increases greatly ($\bar{\tau}/\langle\phi\rangle \to 0$), so that S may have low values, and can tend to zero. The last situation corresponds to very viscous membranes with a low degree of order in which the isotropic limit should be attained

$$\frac{\langle r\rangle}{r_0} = \frac{\langle\phi\rangle}{\bar{\tau}}\cdot\left[1 - \frac{\langle r\rangle}{r_0}\right] \leftrightarrow S = 0.$$

The above analysis shows that if $\langle r\rangle \to r_0$ and if the evolution of $\bar{\tau}/\langle\phi\rangle$ (or of its inverse) is unknown, no conclusion can be drawn from measurement of $\langle r\rangle$ and $\bar{\tau}$ only, i.e., without transient polarized decay studies. On the contrary, if one has any reason to think that the degree of order, S, does not diminish too much when $\langle r\rangle$ increases, S can be estimated by Eq. 19 (33) with the help of approximate values of $\langle\phi\rangle/\bar{\tau}$. In that case, a rather high uncertainty in $\langle\phi\rangle/\bar{\tau}$ will only have a limited effect on the estimated S.

This is why an hypothesis as simple as Jaehnig's (Fig. 2 *b*) works well in the case of a highly ordered system such as DPPC/DPH (Fig. 2 in [33]). The same kind of system is also well described by Van Blitterswijk's fits (1). For the same reason moderately ordered systems ($0.4 < S < 0.8$) give the kind of correlations $\langle r\rangle \leftrightarrow r_\infty$ reported in reference 1; these kinds of correlations are specified in the present report. On the other hand, the system DMPC/cholesterol (3:1) (Fig. 3) deviates considerably from the predictions of Van Blitterswijk et al. and cannot be explained without another hypothesis (see next section). Therefore systems having very low degrees of order and rather high $\langle r\rangle$ ill obey any kind of correlation, probably for experimental reasons, such as low values of $1/\langle\phi\rangle$, which give large uncertainties in high values of $\langle\phi\rangle/\bar{\tau}$, that seriously disturb the use of Eq. 19. These are the cases of the diarachidonyl and dioleyl phospholipids studied by Stubbs et al. (22), but note also that these last systems were unsonicated.

CHOICE OF A SET OF INDEPENDENT VARIABLES AND ITS CONSEQUENCES

This kind of behavior of particular systems led us to propose the following interpretation (38): $\langle\phi\rangle$ (or $1/\langle\phi\rangle$), S, and T never vary independently, and one can define an appropriate surface by the equation

$$\Omega\left[\frac{1}{\langle\phi\rangle}, S, T\right] = 0. \tag{21}$$

Including experiments at constant T (isothermal-cholesterol effects, for instance [39]) and also particular cases with constant degrees of order S, all studies on systems containing DPH are described by a path across the surface. The most frequently given plots in the literature correspond to one of the three possible projections of this path on the reference planes (Fig. 4).

The knowledge of the surface equation $\Omega = 0$ allows us to reduce by one the number of measurements needed to get the parameters of interest, $\langle\phi\rangle$ and S, for, given T and S, $1/\langle\phi\rangle$ becomes derivable from $\Omega = 0$. The method is most

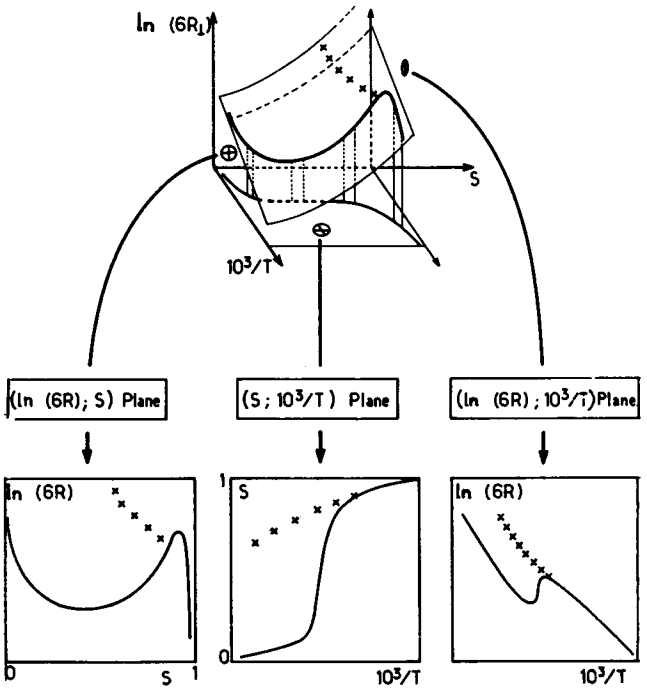

FIGURE 4 The surface relative to the three proposed variables $\langle S\rangle$, T, and $\langle\phi\rangle$ (or $1/\langle\phi\rangle$, or $\ln\langle\phi\rangle, \ldots$) : $\Omega(\langle\phi\rangle, \langle S\rangle, T) = 0$. The path across the surface and its three projections. xxx, behavior of a system such as that described in Fig. 3.

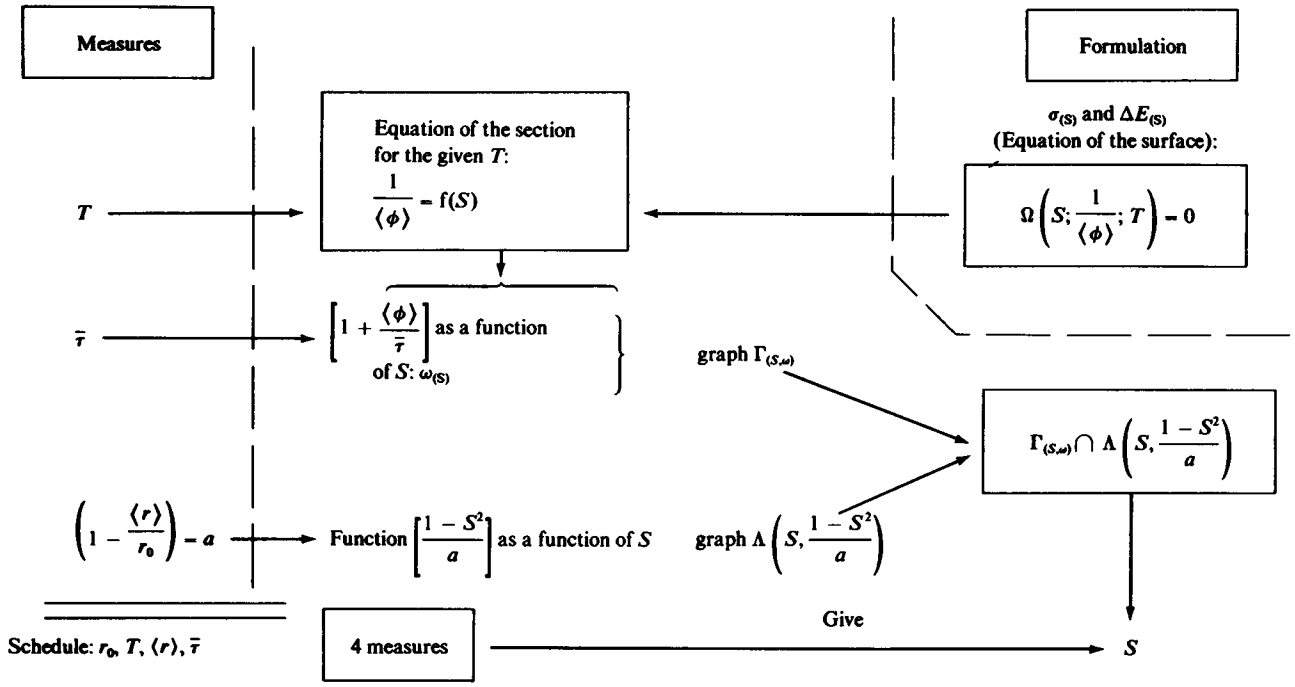

Scheme I

interesting if the surface equation is unique for all membrane systems. As a consequence, measures of $\bar{\tau}$ and $\langle r \rangle$ will once again be sufficient, with the help of the relation, $\Omega = 0$, so that we determine S more accurately than with the different fits previously proposed ($\bar{\tau}$ and $\langle r \rangle / r_0$ alone were also required when an isotropic interpretation of the relaxation of DPH was considered [28–31]). The method for the simplified determination of the degree of order with the help of the Ω function is shown in Scheme I. From the same couple, $\langle r \rangle$ and $\bar{\tau}$, a rather good value of $1/\langle\phi\rangle$ =

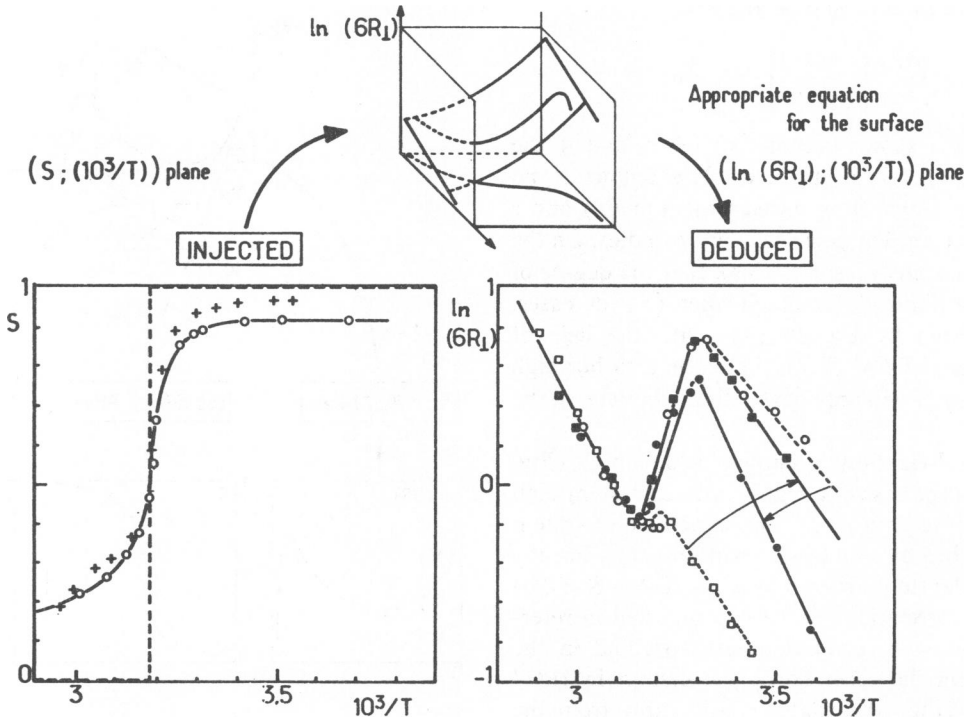

FIGURE 5 Effect of the use of the values of $\langle S \rangle$ measured for DPPC when they are injected into an appropriate equation $\Omega(\langle\phi\rangle, \langle S \rangle, T) = 0$. The consequences are shown in the comparison between the graph (ln $[1/\langle\phi\rangle]$; $10^3/T$) obtained by this method and the different plots of the same graph when derived from separated experiments (reference 6 and 15). ---, experimental values. ——, calculated values.

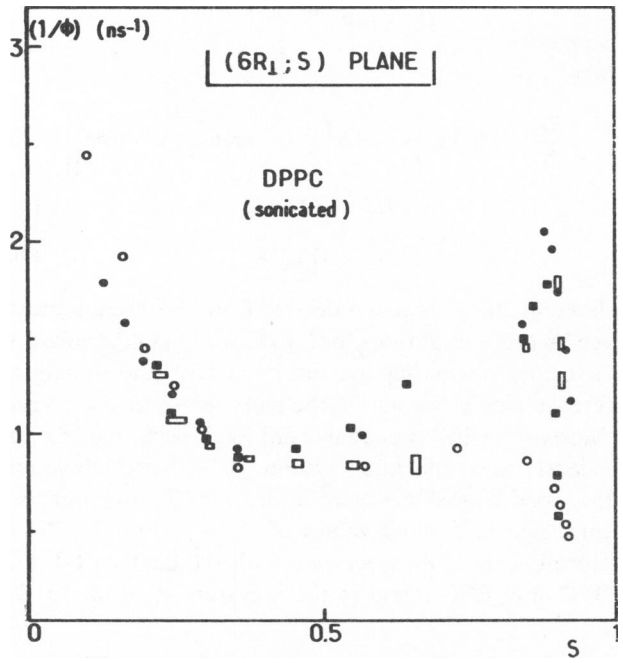

FIGURE 6 Comparison between the graph ($[1/\langle\phi\rangle]$; $\langle S\rangle$) obtained in Fig. 5 with the plots of the same graph derived from the experiments in references 6 and 15. □ and □, values from reference 6. ○, values from reference 15. ■ and ●, values computed from the S values of both references 6 and 15.

$6R_\perp$ can also be estimated, at least in the liquid crystal range of bilayers and in membranes. However, as pointed out above, the use of $\sigma_{(S)}$ in Eq. 11 increases its approximate character, since σ has been defined for the decays of Eq. 3 and not for Eq. 11.

The proposed procedure, summarized in Scheme I, is the following. Because one measures T and, in the same experiment, $\langle r\rangle$ and $\bar{\tau}$, the fixed value of T will reduce Ω, function of the three variables, to $\langle\phi\rangle^{-1} = f(S)$. If Ω is known in analytical form, $f(S)$ and consequently $1 + \langle\phi\rangle/\bar{\tau}$ will be known in analytical form too[2] and can be plotted against S. Let us call $\gamma(S)$ the corresponding curve. In a similar manner, one can draw the function $(1 - S^2)/(1 - \langle r\rangle/r_0)$ as another function of S (curve $\lambda[S]$), because $\langle r\rangle$ is determined. The curves $\gamma(S)$ and $\lambda(S)$ will intersect for a value of S such that

$$\frac{1 - S^2}{1 - \dfrac{\langle r\rangle}{r_0}} = 1 + \frac{\langle\phi\rangle}{\bar{\tau}}, \tag{22}$$

which is equivalent to

$$\frac{r_0(1 - S^2)}{r_0 - \langle r\rangle} - 1 = \frac{\langle\phi\rangle}{\bar{\tau}} \tag{23}$$

or to

$$\langle\phi\rangle^{-1} = \frac{1}{\bar{\tau}} \cdot \left[\frac{r_0 - \langle r\rangle}{\langle r\rangle - r_\infty}\right]. \tag{24}$$

[2] $\bar{\tau}$ here remains the experimental value.

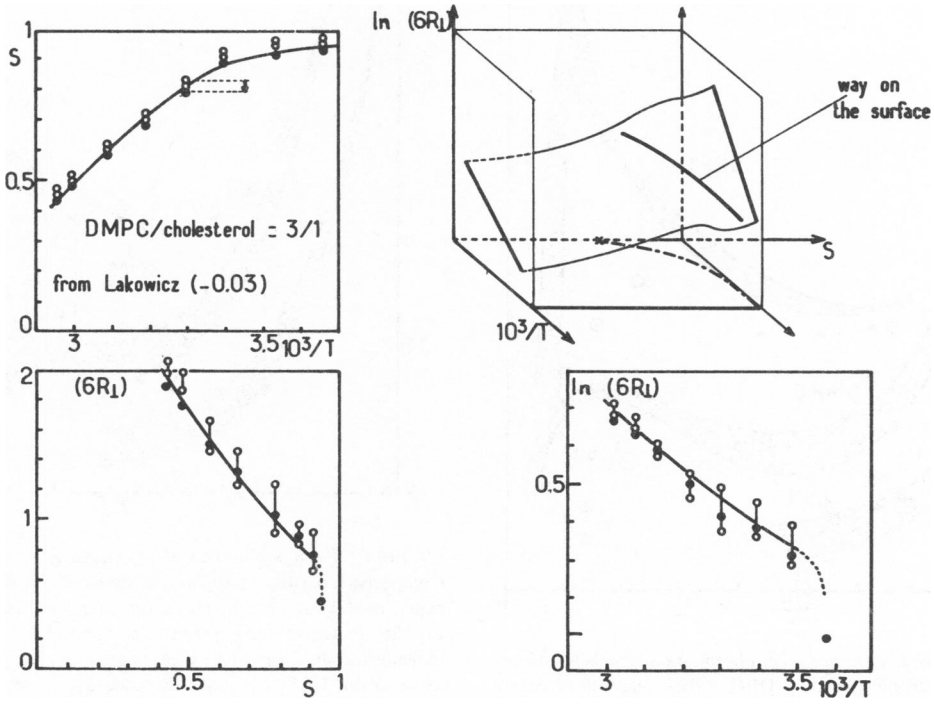

FIGURE 7 The results plotted in Fig. 3 are well now described by the same equation, $\Omega = 0$, as used for DPPC in Fig. 5 and 6. As in Figs. 4 and 5, the experimental values of $\langle S\rangle$ are inserted into the equation of the surface. (A constant value of 0.03 has been subtracted from the values derived from reference 15.) ○, experimental values. ●, computed values.

Consequently, the particular value of S, read for the intersection, will be the degree of order seen by the DPH in the system studied.

POSSIBLE EQUATION FOR THE SURFACE $\Omega\,(1/\langle\phi\rangle, S, T) = 0$

Starting from the relation

$$\frac{1}{\langle\phi\rangle} = \frac{D_\perp}{\sigma(S)} = 6R_\perp \tag{25}$$

and using the experimental results given in references 6, 15, and 22[3] for the DPPC/DPH system, we arrived at the following equations (derived in the Appendix)

$$\sigma(S) = \frac{1}{6}(1 - S^2)(1 - S^4) \tag{26}$$

[3]The last only for comparison, because in that work the samples were not sonicated.

$$D_\perp = D_0 e^{-(\Delta E/\mathcal{R})(1/T - 1/T_0)} \tag{27}$$

where

$$\frac{\Delta E}{\mathcal{R}} = 3300 \times \left\{1 + 0.8\left[\frac{1}{2} + \frac{1}{\pi}\arctan(S - 0.8)\right]\right\} \tag{28}$$

$$D_0 = 0.641\ \text{ns}^{-1} \tag{29}$$

$$T_0 = 373.2°\text{K}. \tag{30}$$

Injecting the values of S derived from the measurements given by previous authors for DPPC (6, 15) in the equation $\Omega = 0$ and projecting the result on both the remaining reference planes, we obtain the plots shown in Figs. 5 and 6. Moreover, when the same operation is performed for the previously nonconforming system (3:1 DMPC/cholesterol), a good consistency can be observed between experimental and calculated values of $1/\langle\phi\rangle$ (Fig. 7). When performing the same operation with the data on DMPC, DOPC, and EPC found in the literature (5, 6, 8, 15, 22,

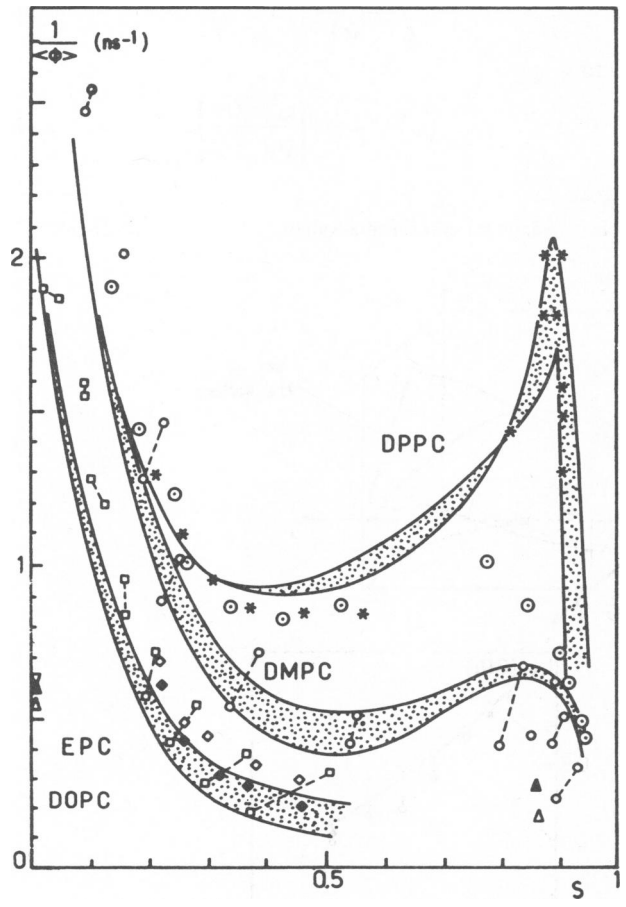

FIGURE 8 Various results obtained with phospholipidic vesicles. Comparison between correlation times of DPH either directly given by experiments or calculated from experimental values of $\langle S \rangle$ with the help of Eqs. 26–30 in text. Points, measures of the cited authors, Kawato et al. (reference 6) and Lakowicz et al. (reference 15). ⊡, calculated values from the $\langle S \rangle$ values given by the same authors.

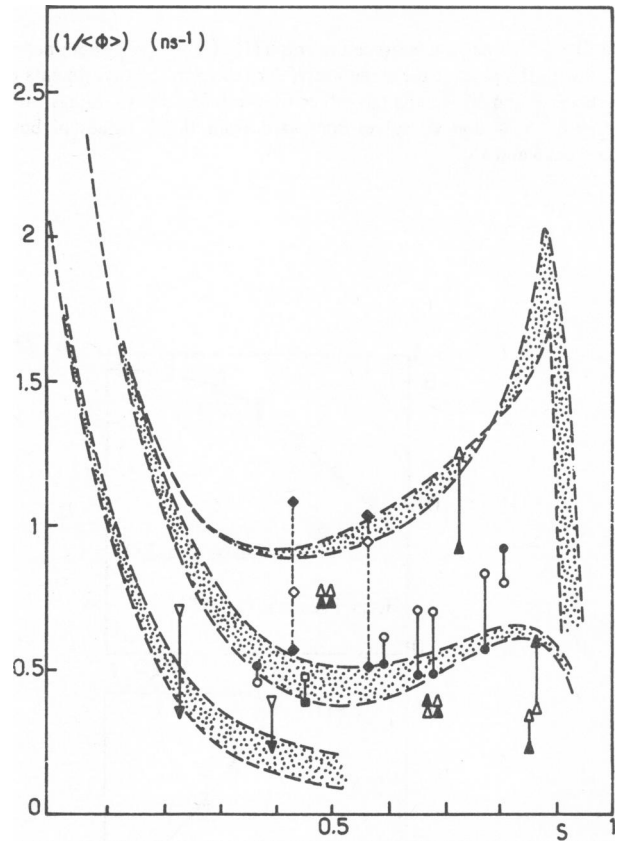

FIGURE 9 Results obtained with various types of natural membranes. Comparison between correlations times of DPH. Full marks indicate experimental data. Empty marks indicate data evaluated with the help of Eqs. 26–29 in text starting from experimental $\langle S \rangle$ values. Dashed areas indicate the three principal sheets determined in Fig. 8. Sources are the same as in Table I: ○—●, reference 39; □—■, reference 40; △—▲, reference 41; ▽—▼, reference 42; ◇—◆, reference 43. Experimental error of $\langle\phi\rangle$ is from 10 to 30% (examples given in Table I). Experimental error of $\langle S \rangle$ is ~[2% × [(1 + $\langle S \rangle$)/$\langle S \rangle$]]. Cumulation of errors on r_∞ and r_0.

39), we once again find the three above mentioned sheets corresponding to the different model systems (Fig. 8). Now, comparisons between the values of $1/\langle\phi\rangle$ given by previous authors in membranes (2, 39–43), and those we obtained by our method (from the S values given by the same authors) become possible. Some of them are shown in Fig. 9 and in Table I (2, 39, 40, 42, 43).

CONCLUDING DISCUSSION

The fact that a single equation holds true for all membrane systems can be contested for very low values of $\langle S\rangle$ in polyunsaturated unsonicated phospholipids (results of Stubbs et al. [22] on diarachidonyl and dioleyl-phosphatidylcholines), but the fact remains that it works remarkably well in most model and membrane systems. We can ask ourselves if this kind of treatment can hold true in the case of rod-shaped molecules fixed at one end, such as the trimethyl-amino-DPH, synthesized and studied by Prendergast and co-workers (44, 45). The answer is relatively easy to find. First, at the theoretical level, the uncorrelated averages, $\langle \mathcal{D}^{(2)}_{0j(t-0)}\rangle \cdot \langle \mathcal{D}^{(2)}_{k0(t-0)}\rangle$, of the Wigner matrix, which determine the squared degree of order (averages taken at the same time) (9–12), correspond, respectively, to the following intervals of integration (10, 44):

$0 \rightarrow 2\pi$ for the Euler angle α,

$0 \rightarrow 2\pi$ for the Euler angle γ,

$0 \rightarrow \pi$ for the Euler angle β.

This last angle characterizes the deviation of the principal molecular axis of the rod with respect to the z-axis of the director, so it appears that either a free rod (such as DPH) or a rod fixed at one end (such as TMA-DPH) will give the same averaged elements, S_{ij}, in a uniaxial environment ($S_{ij} \propto \langle \mathcal{D}^{[2]}_{on} \pm \mathcal{D}^{[2]}_{no}\rangle$ are the elements of the order matrix, see Table I in reference 46).

Second, when the real situation in a phospholipid is examined, it appears that TMA-DPH allows us to explore one-half of the depth of the bilayer only, the half nearer the polar heads. Consequently, this probe gives only a part of the order gradient. Its complement is *trans*-parinaric acid (47–50) because the fluorescent part of this molecule

TABLE I
BIOMEMBRANES ESTIMATION OF CORRELATION TIMES $\langle\phi\rangle$ IN MEMBRANES FROM THE VALUES OF r_∞ MEASURED BY THE CITED AUTHORS WITH HELP OF THE EQUATION $\Omega = 0$*

	Types of biomembranes as cited in corresponding references										
	D17	BHK 21	LM fibroplasts	He-La	N-egg	NDV-MDBK	3T3-A31	SVT2	3T3-d	3T3-Py6	Py 6 R_1
Temperature in °C	25°	25°	25°	25°	25°	25°	37°	37°	37°	37°	37°
used values of $\langle S\rangle$	0.569	0.599	0.65	0.667	0.778	0.804	0.43	0.563	0.514	0.563	0.460
$\frac{1}{\langle\phi\rangle}$ ns^{-1} measured	0.53 ±0.14	0.60 ±0.14	0.48 ±0.15	0.48 ±0.15	0.56 ±0.14	0.91 ±0.4	0.56‡ 1.16§	0.42‡ 1.02§	0.48‡ 1.075§	0.33‡ 0.98§	0.5‡ 1.14§
$\frac{1}{\langle\phi\rangle}$ ns^{-1} calculated from $\langle S\rangle$	0.592	0.628	0.70	0.73	0.83	0.80	0.751	0.923	0.845	0.923	0.780
Reference	39	39	39	39	39	39	43	43	43	43	43

	Types of biomembranes as cited in corresponding references													
	Erythrocytes (human)		Sarcoplasmic reticulum (rabbit)		Mitochondria (rat liver)		Purple membrane *(Halobacterium halobium)*		L 1210	Microsomal extracts (tetrahymena)	
Temperature in °C	10°	35°	10°	35°	10°	35°	10°	35°	25°	15°	39.5°
used values of S	0.861	0.729	0.669	0.491	0.667	0.491	0.854	0.820	0.442–0.575‖	0.394–0.48‖	0.235–0.326‖
$\frac{1}{\langle\phi\rangle}$ ns^{-1} measured	0.625	0.909	0.345	0.769	0.385	0.769	0.204	0.526	0.385	0.238	0.333
$\frac{1}{\langle\phi\rangle}$ ns^{-1} calculated from $\langle S\rangle$	0.37	1.26	0.38	0.758	0.380	0.758	0.357	1.359	0.49–0.60‖	0.311–0.342‖	0.70–0.74‖
Reference	2		2		2		2		40	42	

*Except where stated otherwise, r_0 equals 0.378.
‡$1/\langle\phi\rangle = (\phi_{sub} - 0.704)^{-1}$; the difference takes into account the exciting flash decay (definition of ϕ_{sub} in reference 43).
§Deduced from $\langle r\rangle$, r_0, and r_∞ with $(\langle r\rangle - r_\infty) = 0.03$.
‖With the r_0 value of the cited authors.

generally lies in the other half of the bilayer (32). Comparative results for these dyes would seem to be particularly useful to obtain.

Our procedure is an extension and a much more accurate expression of the method of Van Blitterswijk et al. Even though it exhibits a rather approximate character in some extreme regions of the surface, Ω, its use represents a broadly applicable simplification in the determinations of $\langle S \rangle$ and $1/\langle \phi \rangle = 6R_\perp$ for DPH in model and real membrane systems.

The necessity of taking an $\langle S \rangle$-dependent value of the activation energy of $D_\perp$ neither contradicts the results of Kinosita et al. (2) nor Shinitzky's predictions of a relationship, $\Omega_{SHIN}(6R_\perp, S, T) = 0$. Starting from Eyring's theory of absolute rates, Shinitzky and co-workers proposed that the activation energy of $\langle \phi \rangle^{-1}$ must be an appropriate function of the degree of order (28–31). It is unclear whether this activation energy will be the total or the partial derivative of $\langle \phi \rangle^{-1}$ with respect to T^{-1}. The first case gives

$$\left(\frac{d}{dT}\right) \rightarrow -\left(\frac{\partial \ln D_\perp}{\partial T}\right)_S + \left(\frac{\partial \ln \sigma(S)}{\partial S}\right)_T \cdot \frac{dS}{dT} = \mathcal{F}(S)$$

and the second case

$$\left(\frac{\partial}{\partial T}\right) \rightarrow -\left(\frac{\partial \ln D_\perp}{\partial T}\right)_S = \mathcal{H}(S).$$

In both these relations, one cannot discard a possible dependence of $D_\perp$ on T and/or on S. Whatever the case, it can, consequently, be concluded that the appropriate differential equation can be written in the form

$$\Xi(D_\perp, S, T) = 0,$$

a relationship equivalent to $\Omega(\langle \phi \rangle, S, T) = 0$.

Since Shinitzky's relationship is a differential one, its integration will either give the same result as that which we present here or a different result. This last possibility implies that our path across the surface should be defined by a very small number of constant parameters (transition temperature of the bilayer, slope of $\langle S \rangle$ as a function of T at this temperature, and some other physical constants). We are beginning a similar study with $\langle S^{protein} \rangle$ and $\langle \phi^{protein} \rangle^{-1}$ values we have at hand, the results of which will be given in a subsequent paper.

APPENDIX

To obtain a satisfactory fit to the experimental results,[4] we proceeded in the following manner. (*a*) Various arguments developed by Kinosita et al. (2, 3), Lipari and Szabo (4), and Shinitzky et al. (28–31) led us to consider $\langle \phi \rangle^{-1} = f(S, T)$ as the ratio of a diffusive Arrhenius-type numerator, $\nu(S, T)$, (eventually taken with a S-dependent activation energy) to an appropriate denominator, $\sigma(S)$. (*b*) Because the different models give us various $\sigma(S)$, which could all be approximated by functions such as,

$\sigma(S) \propto 1/6(1 - S) \cdot (1 + S)$	(references 3, 7) (approximated),
$\sigma(S) \propto 1/6(1 - S) \cdot (1 + 2S)$	(reference 1),
$\sigma(S) \propto 1/6(1 - S) \cdot F(S)$	(references 3, 4, 7) ($F[S]$ calculated in reference 4),

we began to build the functions

$$\frac{Z}{\langle \phi \rangle^{-1}} = \left[\frac{\exp \frac{\Delta E}{\mathcal{R}} \left(\frac{1}{T_0} - \frac{1}{T} \right)}{1/6(1 - S^q)} \Bigg/ \langle \phi \rangle^{-1} \right], \qquad \text{(A1)}$$

where as a first approximation we set (*i*) a ΔE independent of S and equal to a numerical value close to that known for $S \rightarrow 0$ in the liquid-crystal state (equal to melted chains) of DPPC and DMPC. In fact, ΔE was incremented around this central value from 6.0 to 8.4 kcal/mol; (*ii*) q successively equal to 1, ½, and 2; (*iii*) T_0 sufficiently high to avoid any problem coming from any residual degree of order in the phase melted at this temperature, $T_0 = 373.2°K \rightarrow 10^3/T_0 = 2.679$.

(*c*) Introducing experimental values of T, S, and $\langle \phi \rangle^{-1}$ found in the literature (6, 15, 22) for the DPPC/DPH system into Eq. A1, we let ΔE and q vary as indicated. We retained the values of those parameters that gave the broadest range for S in which $(Z/\langle \phi \rangle^{-1})$ remained invariant. Those values were $q = 2$ and $\Delta E/\mathcal{R} = 3.3$, resulting in $(Z \cdot \langle \phi \rangle)$ invariant for $0.2 < S < 0.45$. At this step the invariant had the value $D_0^{-1} = Z \cdot \langle \phi \rangle = 1.56$ ns.

Despite this encouraging result, $[Z/(\langle \phi \rangle^{-1})]$ increased slightly from $S = 0.45$ to 0.75, then decreased catastrophically for $S > 0.89$. This meant that $\langle \phi \rangle^{-1}$ increased much faster than Z. Then, because an invariant ratio was wanted, Z had to be divided once again by $(1 - S^w)$. In this operation, the use of a rather high power, w, had two advantages. (*i*) The perturbation introduced into the previously obtained range of invariance of $(Z \cdot \langle \phi \rangle)$ was minimized. (*ii*) There is more opportunity to obtain a satisfactory fit near the limit $S \rightarrow 1$.

(*d*) Because several attempts showed us that this kind of correction was not enough to obtain an invariant ratio, we assumed a corrected function (second approximation) in which, this time, the activation energy was S dependent

$$\frac{Z}{\langle \phi \rangle^{-1}} = \left(\frac{\exp \left\{ 3.3 \times \left[1 + \xi(S) \times \left(2.679 - \frac{10^3}{T} \right) \right] \right\}}{\frac{1}{6}(1 - S^2)(1 - S^w)} \Bigg/ \langle \phi \rangle^{-1} \right). \qquad \text{(A2)}$$

Let us suppose that this fit were to be satisfactory for an appropriate $\xi(S)$. This means that $\xi(S)$ must be equal to

$$\xi(S) = \frac{\ln (0.641) + \ln \langle \phi \rangle - \ln 1/6(1 - S^2)(1 - S^w)}{3.3\left(\frac{10^3}{T} - 2.679 \right)} - 1.$$

This last expression was checked for several values of w. The best sigmoidal curve was obtained for $w = 4$. This value was consequently retained while the sigmoid itself was fitted by an arc tangent function centered at $s = 0.8$ with parameters near those indicated in Eqs. 28–30.

[4]The Appendix was added to answer some questions asked by one of the reviewers. We emphasize above that our equation of the surface is semiempirical and that better fits can still be proposed.

At this stage note that the equation of the surface was determined with the DPPC/DPH system only. By trial and error, we finally determined the parameters of the sigmoid that minimized the residual discrepancies between the obtained Ω and the results corresponding to other phospholipid systems. Obviously, if the analytical forms of Eqs. 26 and 27 are accepted, the best means to derive the optimal numerical values of the parameters it involves would be to use an automatic computing procedure on all the $\{S, T, \langle\phi\rangle\}$ data available in the literature. We have not yet performed this kind of computation because we consider that our analytical form still has too great an empirical character. For instance, it is probable that the activation energy of $D_\perp$ is also a function of the temperature, but we did not succeed in attempting to develop such an interpretation of the results. However, it is particularly encouraging to find that our equation (determined under rather restrictive conditions) is applicable to many different systems.

We thank Dr. M. Kreissler and both the referees for having brought several of the cited works to our attention, also the referees and Dr. J. F. Faucon for pertinent remarks and encouraging discussions.

Received for publication 2 February 1982 and in final form 29 November 1982.

REFERENCES

1. Van Blitterswijk, W. J., R. P. Van Hoeven, and B. W. Van Dermeer. 1981. Lipid structural order parameters (reciprocal of fluidity) in biomembranes derived from steady-state fluorescence polarization measurements. *Biochim. Biophys. Acta.* 644:323–332.
2. Kinosita, K., Jr., R. Kataoka, Y. Kimura, O. Gotoh, and A. Ikegami. 1981. Dynamic structure of biological membranes as probed by 1-6, Diphenyl 1-3-5 hexatriene: a nanosecond fluorescence depolarization study. *Biochemistry.* 20:4270–4277.
3. Kinosita, K., Jr., S. Kawato, and A. Ikegami. 1977. A theory of fluorescence polarization decay in membranes. *Biophys. J.* 20:289–305.
4. Lipari, G., and A. Szabo. 1980. Effect of librational motion on fluorescence depolarization and nuclear magnetic resonance relaxation in macromolecules and membranes. *Biophys. J.* 30:489–506.
5. Chen, L. A., R. E. Dale, S. Roth and L. Brand. 1977. Nanosecond time-dependent fluorescence depolarization of diphenylhexatriene in dimyristoyl-lecithin vesicles and the determination of microviscosity. *J. Biol. Chem.* 252:2163–2169.
6. Kawato, S., K. Kinosita, Jr., S. Kawato, and A. Ikegami. 1977. Dynamic structure of lipid bilayers studied by nanosecond fluorescence techniques. *Biochemistry.* 16:2319–2324.
7. Nordio, P. L., and U. Segre. 1979. Rotational dynamics. *In* The Molecular Physics of Liquid Crystal. G. R. Luckurst and G. W. Gray, editors. Academic Press, New York. 411-426.
8. Dale, R. E., L. A. Chen, and L. Brand. 1977. Rotational relaxation of the microviscosity probe diphenylhexatriene in paraffin oil and egg lecithin vesicles. *J. Biol. Chem.* 252:7500–7510.
9. Szabo, A. 1980. Theory of polarized fluorescent emission in uniaxial liquid crystals. *J. Chem. Phys.* 72:4620–4626.
10. Zannoni, C. 1981. A theory of fluorescence depolarization in membranes. *Mol. Physiol.* 42:1303–1320.
11. Zannoni, C. 1979. A theory of time dependant fluorescence depolarization in liquid crystals. *Mol. Physiol.* 38, 1813–1827.
12. Ehrenberg, M., and R. Rigler. 1972. Polarized fluorescence and rotational brownian motion. *Chem. Phys. Lett.* 14:539–544.
13. Weber, G. 1978. Limited rotational motion: recognition by differential phase fluorometry. *Acta Phys. Pol. Sect. A.* 54:859–865.
14. Lakowicz, J. R., and F. G. Prendergast. 1978. Quantitation of hindered rotation of diphenylhexatriene in lipid bilayers by differential polarized phase fluorometry. *Science (Wash, DC).* 200:1399–1401.
15. Lakowicz, J. R., F. G. Prendergast, and D. Hogen. 1979. Differential polarized phase fluorimetric investigations of diphenylhexatriene in lipid bilayers. Quantitation of hindered depolarizing rotations. *Biochemistry.* 18:508–519.
16. Jarrel, H. C., K. W. Butler, R. A. Byrd, R. Deslauriers, I. Ekiel, and I. C. P. Smith. 1982. ^{2}H-NMR study of *Acholeplasma laidlewii* membranes highly enriched in myristic acid. *Biochim. Biophys. Acta.* 688:622–636.
17. Vogel, H., and F. Jaehnig. 1981. Conformational order of the hydrocarbon chains in lipid bilayers. A Raman spectroscopy study. *Chem. Phys. Lipids.* 29:83–101.
18. Thulborn, K. R., and W. H. Sawyer. 1978. The properties and locations of a set of fluorescent probes sensitive to the fluidity gradient of the lipid bilayer. *Biochim. Biophys. Acta.* 511:125–140.
19. Seelig, A., and J. Seelig. 1974. The dynamic structure of fatty acyl chains in a phospholipid bilayer measured by Deuterium magnetic resonance. *Biochemistry.* 13:4839–4845.
20. Hubbel, W. L., and H. M. McConnell. 1971. Molecular motion in spin labeled phospholipids and membranes. *J. Am. Chem. Soc.* 93:314–326.
21. Straley, J. P. 1976. Theory of piezoelectricity in nematic liquid crystals and the cholesteric ordering. *Phys. Rev. A.* 15:1835–1851.
22. Stubbs, C. D., T. Kouyama, K. Kinosita, and A. Ikegami. 1981. Effect of double bonds on the dynamic properties of hydrocarbon region of lecithin bilayers. *Biochemistry.* 20:4257–4262.
23. Lakowicz, J. R., F. G. Pendergast, and D. Hogen. 1979. Fluorescence anisotropy measurements under oxygen quenching conditions as a method to quantify the depolarizing rotations of fluorophores. D.P.H. in solvents and bilayers. *Biochemistry.* 18:520–527.
24. Lakowicz, J. R., and F. G. Prendergast. 1978. Nanosecond relaxation in membranes observed by fluorescence lifetime. Resolved emission spectra. *J. Biol. Chem.* 254:1771–1774.
25. Lakowicz, J. R., and J. R. Knutson. 1980. Hindered depolarizing rotations of perylene in lipid bilayers. Detection by lifetime-resolved fluorescence anisotropy measurements. *Biochemistry.* 19:905–911.
26. Lakowicz, J. R. 1980. Fluorescence spectroscopic investigations of the dynamic properties of proteins, membranes and nucleic acids. *J. Biochem. Biophys. Methods.* 2:91–119.
27. Johansson, L. B. A., and G. Lindblom. 1980. Orientation and mobility of molecules in membranes studied by polarized light spectroscopy. *Q. Rev. Biophys.* 13:63–118.
28. Shinitzky, M., and Y. Barenholz. 1974. Dynamics of the hydrocarbon layer in liposomes of lecithin and sphingomyelin containing dicetylphosphate. *J. Biol. Chem.* 249:2652–2657.
29. Shinitzky, M., and Y. Barenholz. 1978. Fluidity parameters of lipid regions determined by fluorescence polarization. *Biochim. Biophys. Acta.* 515:367–394.
30. Shinitzky, M., and I. Inbar. 1976. Microviscosity parameters and protein mobility in biological membranes. *Biochim. Biophys. Acta.* 433:133–149.
31. Shinitzky, M., and I. Yuli. 1981. Lipid fluidity at the submacroscopic level; determination by fluorescence polarization. Workshop: Fluorescent Technics and Membrane Markers in Cancerology-Immunology. P. Viallet and C. Rosenfeld, editors. Elsevier Publishing Co. In press.
32. Heyn, M. P. 1979. Determination of lipid order parameters and rotational correlation times for fluorescence depolarization experiments. *FEBS (Fed. Eur. Biochem. Soc.) Lett.* 108:359–364.
33. Jaehnig, F. 1979. Structural order of lipids and proteins in membranes: evaluation of fluorescence anisotropy data. *Proc. Natl. Acad. Sci. USA.* 76:6361–6365.
34. Chapoy, L. L., and D. B. Dupre. 1979. Polarized fluorescence measurements of orientational order in a uniaxial liquid crystal. *J. Chem. Phys.* 70:2550–2553.

35. Chapoy, L. L., and D. B. Dupre. 1978. Polarized fluorescent emission in uniaxial liquid crystals. The effect of intramolecular energy transfer and rotational Brownian motion on measurements of the orientational distribution function. *J. Chem. Phys.* 69:519–524.
36. Yguerabide, J., and M. C. Foster. 1981. Fluorescence spectroscopy of biological membranes. *In* Membrane Spectroscopy. E. Grell, editor. Springer Verlag, Berlin. 31.
37. Lentz, B. R., B. M. Moore, and D. A. Barrow. 1979. Light scattering effects in the measurement of membrane microviscosity with diphenylhexatriene. *Biophys. J.* 25:489–494.
38. Hare, F. 1981. Correlations between fluidity and degree of order estimated by fluorescence depolarization in models and membranes exhibiting or not a thermal transition. Workshop: Fluorescent Technics and Membrane Markers in Cancerology-Immunology. Elsevier Publishing Co. In press.
39. Hildenbrand, K., and C. Nicolau. 1979. Nanosecond fluorescence anisotropy decays of 1-6 diphenyl 1-3-5 hexatriene in membranes. *Biochim. Biophys. Acta.* 553:365–377.
40. Sene, C., D. Genest, A. Obrenovitch, P. Wahl, and M. Monsigny. 1978. Pulse fluorimetry of 1-6 diphenyl 1-3-5 hexatriene incorporated in membranes of mouse leukemic L 1210 Cells. *FEBS (Fed. Eur. Biochem. Soc.) Lett.* 88:181–186.
41. Kinosita, K., Jr., S. Kawato, A. Ikegami, and S. Yoshida. 1981. The effect of cytochrome oxidase on lipid chain dynamics. A nanosecond fluorescence depolarization study. *Biochim. Biophys. Acta.* 647:7–17.
42. Martin, C. E., and D. C. Foyt. 1978. Rotational relaxation of 1-6 diphenyl hexatriene in membrane lipids of cells acclimated to high and low growth temperatures. *Biochemistry.* 17:3587–3591.
43. Parola, A. H., P. W. Robbins, and E. R. Blout. 1979. Membrane dynamic alterations associated with viral transformation and reversion. *Exp. Cell Res.* 118:205–214.
44. Engel, L. W., and F. G. Prendergast. 1981. Values for and significance of order parameters and "cone angles" of fluorophore rotation in lipid bilayers. *Biochemistry.* 20:7338–7345.
45. Prendergast, F. G., R. P. Haugland, and P. J. Callahan. 1981. 1-[4 Trimethylaminophenyl] 6 phenyl hexa 1-3-5 triene: synthesis, fluorescence properties and use as a probe of lipid bilayers. *Biochemistry.* 20:7333–7338.
46. Polnaszek, C. F., and J. H. Freed. 1975. ESR studies of anisotropic ordering, spin relaxation and slow tumbling in liquid crystalline solvents. *J. Phys. Chem.* 79:2283–2306.
47. Wolber, P. K., and B. S. Hudson. 1981. Fluorescence lifetime and time resolved polarization anisotropy studies of acyl chain order and dynamics in lipid bilayers. *Biochemistry.* 20:2800–2810.
48. Sklar, L. A., and E. A. Dratz. 1980. Analysis of membrane bilayer asymmetry using parinaric acid fluorescent probes. *FEBS (Fed. Eur. Biochem. Soc.) Lett.* 118:308–310.
49. Sklar, L. A., G. P. Miljanich, and E. A. Dratz. 1979. Phospholipid lateral phase separation and the partition of cis and trans-parinaric acid among aqueous, solid lipid and fluid lipid phases. *Biochemistry.* 18:1707–1716.
50. Tecoma, E. S., L. A. Sklar, R. D. Simoni, and B. S. Hudson. 1977. Conjugated polyene fatty acids as fluorescent probes: biosynthetic incorporation of parinaric acid by *Escherichia Coli,* and studies of phase transitions. *Biochemistry.* 16:829–835.